A Runge-Kutta Discontinuous Galerkin Solver for 2D Boltzmann Model Equations: Verification and Analysis of Computational Performance

Wei Su[a,b], Alina A. Alexeenko[b] and Guobiao Cai[a]

[a]*School of Astronautics, Beihang University, Beijing, 100191, P.R. China*
[b]*School of Aeronautics & Astronautics, Purdue University, West Lafayette, IN, 47907, USA*

Abstract. The high-order Runge-Kutta discontinuous Galerkin (DG) method is extended to the 2D kinetic model equations describing rarefied gas flows. A DG-type discretization of the equilibrium velocity distributions is formulated for the Bhatnagar-Gross-Krook and ellipsoidal statistical models which enforce a weak conservation of mass, momentum and energy in the collision relaxation term. The RKDG solutions have up to 3rd-order spatial accuracy and up to 4th-order time accuracy. Verification is carried out for a steady 1D Couette flow and a 2D thermal conduction problem by comparison with DSMC and analytical solutions. The computational performance of the RKDG method is compared with a widely used second-order finite volume method.

Keywords: high-order Discontinuous Galerkin (DG), deterministic methods, model equations.
PACS: 02.60.Cb, 47.11.Fg, 47.45.-n

INTRODUCTION

In a wide range of applications, non-equilibrium rarefied gas flows require simulation with accurate and efficient computational methods and aerothermodynamics models. The governing equation for rarefied gas flows at arbitrary Knudsen numbers is the Boltzmann equation, which includes a complex nonlinear collision term. Two broad categories for the numerical solutions of the Boltzmann-based equations are stochastic approaches and deterministic methods. The direct simulation Monte Carlo (DSMC) method [1] is a stochastic approach that has been widely applied to analyze high-speed rarefied flows. A major shortcoming of the DSMC method is the high computational cost for near the continuum and low-speed flows. In addition, the stochastic particle-based approach is less suitable for unsteady flow simulations.

An alternative approach is the deterministic numerical simulation of the full Boltzmann or kinetic model equations with a simplified collision term model. Two of the often-used forms of model kinetic equations are the Bhatnagar-Gross-Krook (BGK) [2] and the ellipsoidal statistical BGK (ES-BGK) [3] models. Although the deterministic solutions have shown significant improvement in numerical efficiency, especially in low-speed micro-scale flows, the multi-dimensionality of the equations in phase space makes the approach demanding in terms of CPU time and memory. Therefore, high-order numerical schemes are desirable for expanding the scope of rarefied flow problems that can be solved accurately. Recent approaches for spatial discretization include finite difference method (FDM) [4, 5, 6], finite volume method (FVM) [7] and Runge-Kutta discontinuous Galerkin (RKDG) method [8, 9]. Both explicit [4, 5] and implicit schemes [4, 7, 10, 11] have been implemented for the time discretization in the FDM and FVM methods.

The RKDG method is a finite element method [12], which is well suited for the solution of time-dependent hyperbolic and advection dominated equations. Compared to other high-order methods like FVM or FDM, this method can obtain solutions with arbitrarily high-order accuracy with relatively small cost. Other advantages include easy formulation of boundary conditions and efficient parallel implementation. The RKDG method has been applied for the 1D/1V kinetic models [8]. In this work, we extend the conservative formulation of RKDG to 2D/2V and 2D/3V formulations of model kinetic equations. Two steady problems are used to verify the proposed solver and comparisons with an FVM solver are performed in order to analyze its computational efficiency.

KINETIC MODELS

The kinetic model equations are written as

28th International Symposium on Rarefied Gas Dynamics 2012
AIP Conf. Proc. 1501, 381-388 (2012); doi: 10.1063/1.4769547

$$\frac{\partial f}{\partial t} + \boldsymbol{c} \cdot \frac{\partial f}{\partial \boldsymbol{r}} = \nu (f_E - f), \tag{1}$$

where, f is the molecular velocity distribution function, while $\boldsymbol{c}$ and $\boldsymbol{r}$ are the velocity and spatial coordinates. In BGK model f_E is the local Maxwell distribution, and in ES-BGK model f_E is a local anisotropic Gaussian, ν is the collision frequency given as

$$\nu = \begin{cases} \dfrac{P}{\mu} & BGK\ Model \\ Pr\dfrac{P}{\mu} & ES-BGK\ Model \end{cases}, \tag{2}$$

where P is the pressure, μ is the viscosity coefficient assumed here in a power-law form $\mu=\mu_{ref}(T/T_{ref})^{\omega}$, with μ_{ref}, T_{ref} and ω given by Bird [1]. Pr is the Prandtl number, taken as 2/3 for a monatomic gas. For 2D/2V cases, two reduced distribution functions are introduced to reduce the computational cost

$$f_1(t,x,y,c_x,c_y) = \int_{-\infty}^{\infty} f(t,x,y,\vec{c})\,dc_z, \qquad f_2(t,x,y,c_x,c_y) = \int_{-\infty}^{\infty} c_z^2 f(t,x,y,\vec{c})\,dc_z. \tag{3}$$

Finally, the governing equations are obtained as

$$\frac{\partial f_p}{\partial t} + c_x \frac{\partial f_p}{\partial x} + c_y \frac{\partial f_p}{\partial y} = \nu (f_{E,p} - f_p), \quad p = 0,1 \text{ or } 2, \tag{4}$$

where p =0 denotes the full distribution function for 3V cases.

NUMERICAL METHOD

The model equations are first discretized in the velocity space. Both Cartesian and spherical type meshes are used [11]. The Cartesian type is easy to implement, however, the finite limits on the velocity space must be chosen carefully to ensure that transport processes for velocities outside the target range have a negligible effect. The spherical type is well suited for highly non-equilibrium flows. Gaussian-Laguerre quadrature up to 16th order in velocity magnitude and both 3/8th Simpson rule and constant interval in angles have been applied here. The velocity nodes are stored in an array, where $\boldsymbol{c}^j$ is the j^{th} element of the array. If we denote $f_p^j(t,x,y)=f(t,x,y,\boldsymbol{c}^j)$, the model equations are transformed into a system of equations

$$\frac{\partial f_p^j}{\partial t} + c_x^j \frac{\partial f_p^j}{\partial x} + c_y^j \frac{\partial f_p^j}{\partial y} = \nu (f_{E,p}^j - f_p^j). \tag{5}$$

The macroscopic parameters are calculated through numerical quadrature of the corresponding moments of velocity distribution functions.

Discontinuous Galerkin Formulation and Time Discretization

We use the discontinuous Galerkin method to discretize the system on both structured and unstructured triangle-type spatial meshes. The approximate solutions of f_p^j are sought in the finite element space of piecewise functions within each triangle K_i [12]

$$f_p^j(t,x,y) = \sum_{l=1}^{k} F_{p,i}^{j,l}(t)\varphi_i^l(x,y), \tag{6}$$

where, $\varphi_i^l(x,y)$ is the basis function supported in triangle K_i and k is the total number of the basis functions, while $F_{p,i}^{j,l}(t)$ is the respective degree of freedom. In this work, we present the piecewise linear and piecewise quadratic approximations with 2nd-order and 3rd-oder spatial accuracy, respectively. For the 2nd-order case, the three basis functions are the linear functions which take the value 1 at one of the midpoints of the edges of K_i and the value 0 at the midpoints of the other two edges. For the 3rd-order case, the basis functions are the quadratic functions which take the value 1 at one of the six points (the three midpoints of edges and three vertices) in K_i and value 0 at the remaining five points.

In order to determine the degrees of freedom, the standard techniques of the finite element formulations are applied to obtain the weak formulation of the governing system of equations, which is expressed as

$$\sum_{l=1}^{k} M_{ml} \frac{d}{dt} F_{p,i}^{j,l}(t) + \sum_{e \in \partial K_i} \int_e h_{e,K_i}(x,y,t) \varphi_i^m(x,y) d\Gamma - c_x^j \sum_{l=1}^{k} F_{p,i}^{j,l} Q_{ml}^x - c_y^j \sum_{l=1}^{k} F_{p,i}^{j,l} Q_{ml}^y$$
$$= \int_{K_i} \nu (f_{E,p}^j - \sum_{l=1}^{k} F_{p,i}^{j,l} \varphi_i^l(x,y)) \varphi_i^m(x,y) dxdy \quad m = 1,...,k. \tag{7}$$

where, $h_{e,Ki}(x,y,t)$ is the numerical flux at the edge e of the triangle K_i, with the matrice M_{ml} and Q_{ml} are defined as

$$M_{ml} = \int_{K_i} \varphi_i^m(x,y) \varphi_i^l(x,y) dxdy, \tag{8}$$

$$Q_{ml}^x = \int_{K_i} [\frac{\partial}{\partial x} \varphi_i^m(x,y)] \varphi_i^l(x,y) dxdy, Q_{ml}^y = \int_{K_i} [\frac{\partial}{\partial y} \varphi_i^m(x,y)] \varphi_i^l(x,y) dxdy. \tag{9}$$

Finally, the resulting system of ordinary differential equations (ODEs) is discretized in time by a special class of explicit total variation diminishing (TVD) Runge-Kutta schemes [13].

Numerical Flux and Boundary Conditions

The values of f_p^j have discontinuities at the edges of the triangles. Two-point Lipschitz numerical fluxes are used to approximate the exact fluxed [12]. In this work, this simple upwind flux is applied

$$h_{e,K_i}(x,y,t) = \begin{cases} \boldsymbol{c}^j \cdot \boldsymbol{n}_{e,K_i} f_p^j(int(K_i),t), & \boldsymbol{c}^j \cdot \boldsymbol{n}_{e,K_i} \geq 0 \\ \boldsymbol{c}^j \cdot \boldsymbol{n}_{e,K_i} f_p^j(ext(K_i),t), & \boldsymbol{c}^j \cdot \boldsymbol{n}_{e,K_i} < 0 \end{cases}, \tag{10}$$

where $f_p^j(int(K_i),t)$ is the approximate solution obtained from the interior of the triangle K_i and $f_p^j(ext(K_i),t)$ is the one obtained from the exterior of K_i. $\boldsymbol{n}_{e,Ki}$ is the outward unit normal to the edge e.

The boundary values $f_p^j(ext(K_i),t)$ should be specified at the boundary edges. Five different types of boundary conditions are incorporated into the solver, which include: symmetry boundary, specular-diffuse moving wall with a given accommodation coefficient, periodic boundaries, far pressure inlet/outlet boundaries, and supersonic inlet/outlet boundaries.

Conservative Discretization of the Collision Term

The discrete equilibrium distribution functions $f_{E,p}^j$ are evaluated at each intermediate step of the Runge-Kutta process such that the conservations of mass, momentum and energy are enforced in the collision relaxation term. For the BGK model, $f_{E,p}^j$ are defined as

$$f_{E,0}^j = \exp[a_1 - a_2(\boldsymbol{c}^j - \boldsymbol{u}) + a_3(c_x^j - u) + a_4(c_y^j - v)]. \tag{11}$$

For the ES-BGK model, $f_{E,p}^{j}$ are defined as

$$f_{E,0}^{j} = \exp[a_1 - a_2(c_x^j - u) + a_3(c_x^j - u) - a_4(c_y^j - v)^2 + a_5(c_y^j - v) + a_6 c_x^j c_y^j - a_7 c_z^{j2}] \tag{12}$$

Here, ***u(u,v)*** is the macroscopic flow velocity.

In order to be consistent with the weak formulation of the DG method and to retain high order accuracy, the coefficients as are sought with the form

$$a_s(x,y) = \sum_{l=1}^{k} A_s^l \varphi_i^l(x,y). \tag{13}$$

The difference between this form and the one used in the FVM method is that the collision frequency and other macro properties can vary inside the spatial elements. The unknown coefficients A_s^l are obtained from the weak formulation of mass, momentum and energy conservation for the collision relaxations [8]. The obtained non-linear system of equations is solved using Newton's method. In this way, the discrete collision term does not give rise to any source or sink of mass, momentum or energy.

RESULTS AND DISCUSSIONS

Verification of the numerical solution of Boltzmann kinetic model equations with the RKDG method formulations in 2D/2V and 2D/3V is carried out by comparison with analytical solutions for a 1D and 2D steady flow problems. The RKDG solution is compared with analytical formulas and the DSMC solution as well as numerical solutions by a finite-volume solver [7]. For convenience, the notations of the numerical method are illustrated in Table 1. The entire set of tests is done in double precision on the CARTER parallel cluster in Purdue University. Specially, the queue has 4 nodes with two 8-Core Intel Xeon-E5 processors and 32GB RAM per nodes.

TABLE 1. Notations of the Numerical Methods Used in this Work.

Notation	Numerical method
DSMC	The direct simulation of Monte Carlo method
FVM-2	FVM with 2nd order minmod flux combined with 2nd order time integration
RKDG-2	2nd order DG method with 2nd order RK time integration
RKDG-3	3rd order DG method with 3rd order RK time integration

Verification: One-Dimensional Compressible Couette Flow

The first test case considered is the one-dimensional planar compressible Couette flow calculated on 2D meshes. The argon gas is bounded by two plates H=1.0 m apart maintained at a temperature of T_w=273 K. The bottom wall is at rest while the top one is moving with the velocity u_w=300 m/s in the x direction. Initially the gas has a density ρ_0=9.28×10^{-6} kg/m^3 corresponding to the Knudsen number from the variable hard sphere model as 0.00925. For the cases Kn=0.0925 and Kn=0.925, all the conditions are same except the gas densities are ρ_0=9.28×10^{-7} kg/m^3 and ρ_0=9.28×10^{-8} kg/m^3, respectively.

The 2D/3V numerical solutions were conducted for both the BGK and ES-BGK models. The steady-state solution was obtained by iterating in time until the time convergence was reached. The time convergence criterion is that the L_2 norm of the change of density and temperature per time step

$$\sqrt{\int_K (Q_{new} - Q_{old})^2 dxdy \Big/ \int_K Q_{old}^2 dxdy} \,/\, dt, \tag{14}$$

are less than 10^{-6}, where Q_{new} is the macro parameters obtained at the current time step and Q_{old} is the ones obtained at the previous step.

The schematic of the spatial mesh for RKDG and FVM methods is illustrated in Fig. 1. The triangle type mesh was used in RKDG simulation, and the Cartesian type mesh was used in FVM simulation. For RKDG cases, the west and east boundaries were periodic boundary condition, while the zero-gradient boundary condition was utilized in FVM cases. In this 1D problem, the two conditions are equivalent. The specular-diffuse moving wall with a given accommodation coefficient is used on the upper and lower walls. Cartesian type of velocity mesh were applied with

$10\times10\times10$ nodes for Kn=0.00925 case, and $20\times20\times20$ nodes for the other cases. The CFL numbers of about 0.3, 0.25 and 0.6 were applied for RKDG-2, RKDG-3 and FVM-3 respectively. All the cases were run on a single processor. The BGK solutions of bulk velocities are plotted in Fig. 2. N_y denotes the cell (triangle or rectangle) numbers along y direction. The very good agreements between the RKDG solutions and the DSMC results show the ability of the solver for rarefied flow with variable Kn numbers and wall conditions with variable accommodation coefficients. The big difference between the BGK solutions and ES-BGK solutions is the temperature profiles, which is due to the fact that the ES-BGK model gives a correct Pr number.

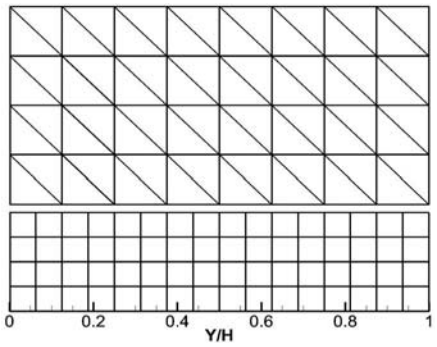

FIGURE 1. Schematic of the spatial meshes. The top triangle mesh is used in RKDG simulations, and the bottom Cartesian mesh is used in FVM simulations.

For comparison of the computational efficiency of the methods, the time interval, number of iteration, number of computation nodes and total CPU times are listed in Table 2. The RKDG method in general is more CPU intensive than the FVM-2 method for the same number of cells. The most computationally intensive part is the calculation of the equilibrium distribution functions in the collision relaxation term [8]. This is the reason that the solution of the ES-BGK models requires more time than that of the BGK solution (about 3 times). In addition, the DG method requires smaller time steps than the FV method. Based on the comparisons of the bulk velocity with the DSMC results, the RKDG-2 solution with N_y=8 and the RKDG-3 solution with N_y=4 are at least as good as FVM-2 with N_y=128. This indicates that the DG method is more efficient in the discretization of the physical space. The CPU times for the RKDG-2 solution with N_y=8 are about 5 times less than that for the FVM solution with N_y=128 for the BGK model. The required memory is also about 5 times less. In general, the RKDG-2 solution requires significantly less memory and CPU time than FVM-2 with the same accuracy. The RKDG-3 method is not more efficient than the FVM-2 due to the smaller time steps are required. Note that the stencil of the DG method only involves the closest neighbor cells, which allows for more efficient domain decomposition in parallel computations.

TABLE 2. Computational Parameters for Different Methods and Models for Couette flow.

Solution	Mesh	Δt, sec	# of iterations	CPU time, h	RL_1error, %	RL_2error, %
BGK	4×2	5×10^{-5}	1,357	0.08	12.14	7.20
RKDG-2	4×4	3×10^{-5}	15,831	1.70	2.51	1.93
	4×8	2×10^{-5}	18,514	3.83	0.72	0.42
	4×16	1×10^{-5}	36,593	14.55	0.51	0.23
	4×32	8×10^{-6}	52,333	40.98	0.50	0.22
ES-BGK	4×2	5×10^{-5}	1,360	0.33	12.36	7.20
RKDG-2	4×4	4×10^{-5}	11,979	5.30	2.47	1.92
	4×8	2×10^{-5}	17,899	14.94	0.70	0.42
	4×16	1×10^{-5}	35,027	58.18	0.41	0.19
BGK	4×2	3×10^{-5}	17,155	10.71	3.05	1.88
RKDG-3	4×4	2×10^{-5}	18,553	20.86	0.65	0.37
	4×8	1×10^{-5}	36,667	84.863	0.50	0.25
BGK	4×16	2×10^{-5}	10,295	0.32	13.74	7.93
FVM-2	4×32	1×10^{-5}	29,263	1.72	7.66	3.66
	4×64	8×10^{-6}	42,614	5.25	2.96	1.22
	4×128	4×10^{-6}	89,693	20.57	1.04	0.38

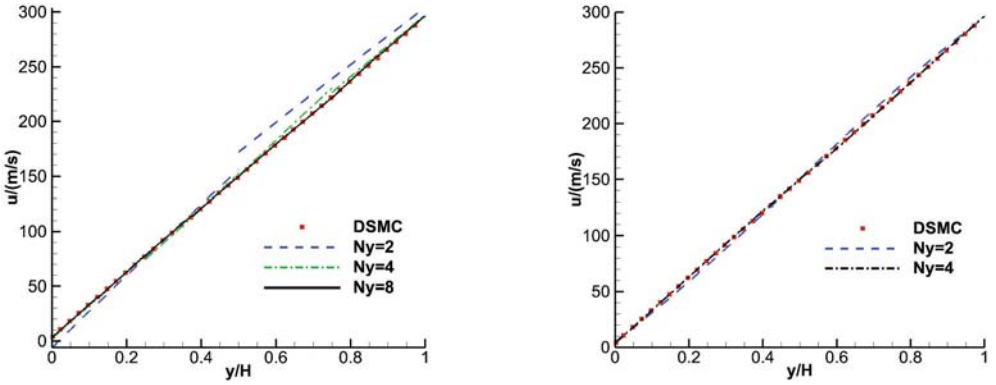

(a) BGK RKDG-2 solutions with Kn=0.00925, α=1.0 (b) BGK RKDG-3 solutions with Kn=0.00925, α=1.0

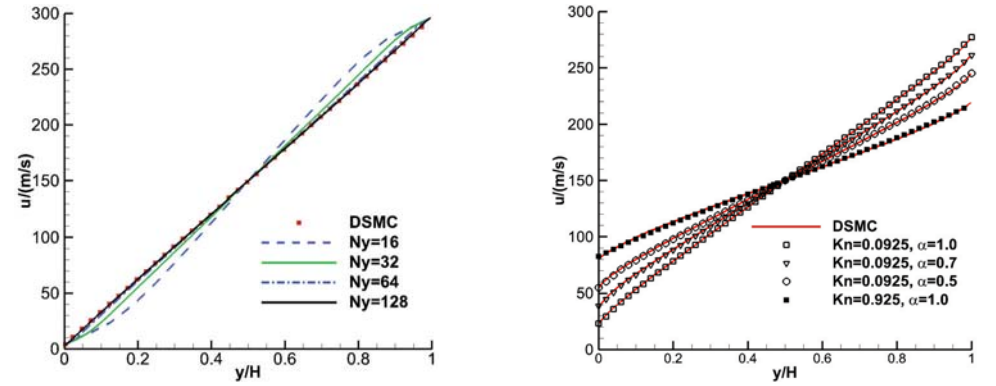

(c) BGK FVM-2 solutions with Kn=0.00925, α=1.0 (d) BGK RKDG-2 solutions with variable Kn and α

FIGURE 2. Calculated bulk velocities for BGK solutions of Couette flow with different numerical methods

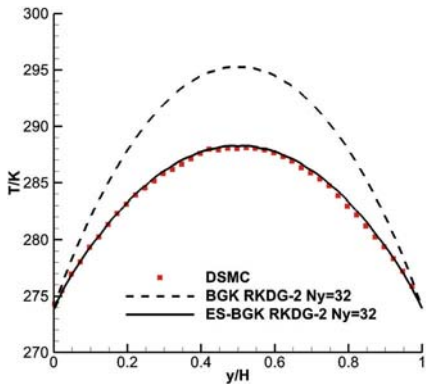

FIGURE 3. Calculated temperature for RDKG-2 solution for different models with Kn=0.00925, α=1.0

Verification: Two-Dimensional Thermal Conduction

The second verification is carried out for a steady two-dimensional thermal conduction problem with three boundaries maintained at T_1=273.15 K, while the fourth side is maintained at T_2=327.78 K. The Argon gas is initialized with temperature T_1, and density $\rho=4.77\times10^{-4}$ kg/m^3, corresponding to a Knudsen number of 0.0018. The 2D/2V RKDG method was applied for the ES-BGK model. Solutions were sought on the domain of 0.05×0.1 m, with four different spatial meshes including an unstructured mesh. The symmetry boundary is used at x=0.05 m. Spherical type of velocity mesh with 3/8th Simpson rule consisting of 8 nodes in velocity magnitude and 12 nodes in velocity angle were used.

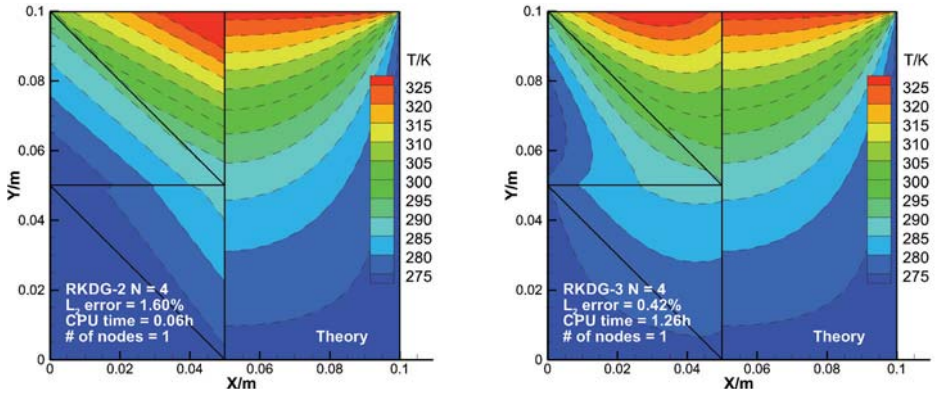

(a) RKDG-2 solutions on 4 triangles (b) RKDG-3 solutions on 4 triangles

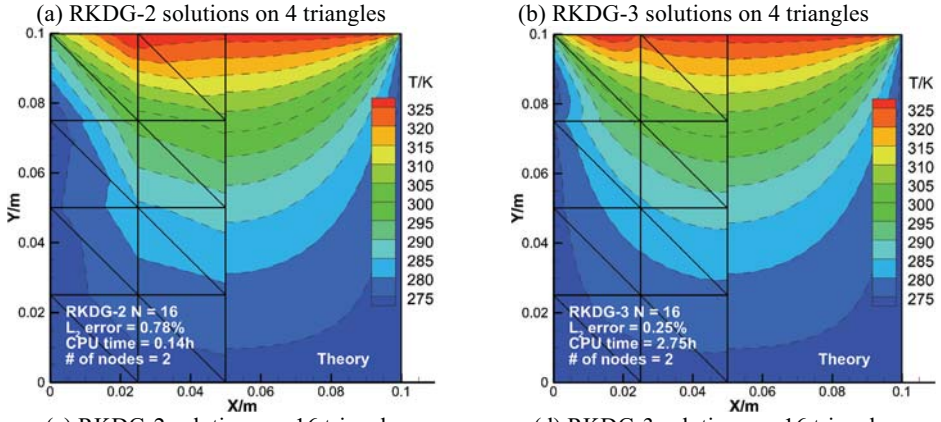

(c) RKDG-2 solutions on 16 triangles (d) RKDG-3 solutions on 16 triangles

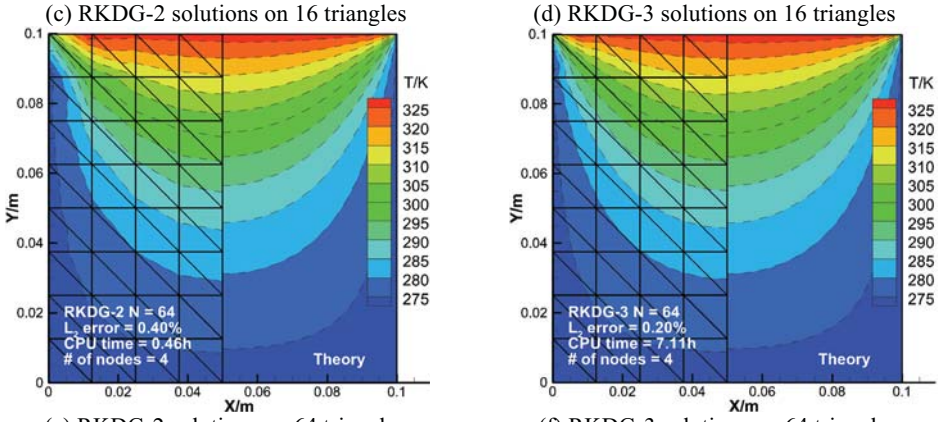

(e) RKDG-2 solutions on 64 triangles (f) RKDG-3 solutions on 64 triangles

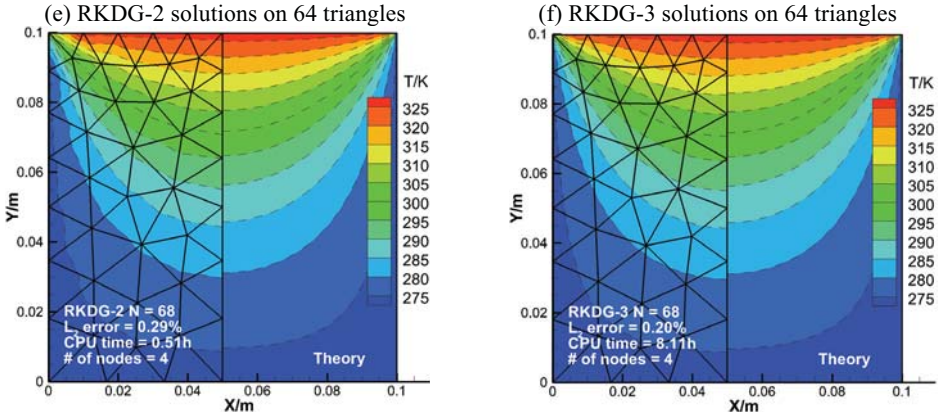

(g) RKDG-2 solutions on 68 triangles (h) RKDG-3 solutions on 68 triangles

FIGURE 4. Comparison of RKDG solutions on different meshes for a 2D thermal conduction problem

Time convergence was reached when the L_2 norms of the density and temperature residuals are less than 10^{-7}. The theoretical solution is given as [14]

$$\theta(x,y) = \frac{2}{\pi}\sum_{n=1}^{\infty}\frac{(-1)^{n+1}+1}{n}\sin(\frac{n\pi x}{L})\cdot\sinh(\frac{n\pi y}{L})\Big/\sinh(\frac{n\pi W}{L}), \tag{15}$$

where θ is the normalized temperature as. L and W are respectively the length and width of the plate. Calculated temperature contours compared with the theoretical solution are plotted in Fig. 4. Good agreements are observed between the RKDG solutions and the theoretical solution. To study convergence, the L_2 norm errors are estimated for each case. The theoretical result is used as the exact solution. The CPU time and the number of nodes are also illustrates for each case. Comparison shows that, for the same convergence level, the RKDG-3 method uses at least 16 times fewer cells than that of RKDG-2 method. Therefore, with same spatial elements, the RKDG-3 method obtains much better results than that of RKDG-2 method. However, as mentioned above, it requires larger CPU time and memory.

CONCLUSIONS

The high-order RKDG method has been extended to 2D/2V and 2D/3V Boltzmann model equations. In this approach, the velocity space is firstly discretized using either Cartesian or spherical type discrete velocity methods. Then, the discrete partial differential equations are discretized on spatial triangle-type meshes using the discontinuous Galerkin (DG) method. The linear and quadratic functions are chosen as the basis functions respectively for the second-order and third-order DG method. The system of ordinary differential equations, which is obtained from the spatial discretization, is finally discretized in time using a special class of explicit Runge-Kutta time discretization methods. At each intermediate step of the RK process, the equilibrium velocity distribution function in the model equations is estimated using a discontinuous conservative discretization method, which enforces a weak conservation of mass, momentum and energy for the collision relaxation term. Verification of the formulation and solver has been performed by comparison with DSMC and analytical solutions for rarefied compressible Couette flow and near-continuum 2D thermal conduction problem. Results show that, with the same accuracy, RKDG-2 solution requires significantly less memory and CPU time than that of FVM-2 method.

ACKNOWLEDGMENTS

The authors wish to thank the China Scholarship Council for the support of Wei Su's visiting study at Purdue University. The authors also want to thank Dr. A. Venkattraman of Purdue University for his valuable help with DSMC and FVM simulations.

REFERENCES

1. G. A. Bird, *Molecular Gas Dynamics and the Direct Simulation of Gas Flows 2nd ed*, Oxford: Clarendon press, 1994.
2. P. L. Bhatnagar, E. P. Gross and M. Krook, *Phys. Rev.* **94**, 511-525 (1954).
3. H. L. Holway, *Phys. Fluids* **9**, 1658-1673 (1966).
4. J. Y. Yang and J. C. Huang, *J. Comput. Phys*. **120**, 323-339 (1995).
5. Z. H. Li and H. X. Zhang, *Int. J. Numer. Method Fluids.* **42**, 361-382 (2003).
6. V. I. Kolobov, R. R. Arslanbekov, V. V. Aristov, A. A. Frolova and S. A. Zabelok, *J. Comput. Phys.* **223**, 589-608 (2007)
7. L. Mieussens and H. Struchtrup, *Phys Fluids.* **16**, 2797-2813 (2004).
8. A. A. Alexeenko, C. Galitzine and A. M. Alekseenko, *AIAA Paper,* No. 2008-4256 (2007).
9. L. L. Baker and N. G. Hadjiconstantinou, *Int. J. Numer. Method Fluids.* **58**, 381-402 (2008).
10. V. A. Titarev, *Commun. Comput. Phys*. **12**, 161-192 (2012).
11. S. Chigullapalli and A. A. Alexeenko, *AIAA Paper,* No. 2011-3993 (2011).
12. B. Cockburn and C. W. Shu. *J. Comput. Phys.* **141**, 199-224 (1998).
13. C. W. Shu and S. Osher. *J. Comput. Phys.* **77**, 439-471 (1988).
14. F. P. Incropera, *Fundamentals of Heat and Mass Transfer 6th ed*. Hoboken: John Wiley, 2007.